

The role of protons in the NO reduction by acetylene over ZSM-5

Qing Yu, Xiping Wang*, Na Xing, Hongliang Yang, Shixin Zhang

State Key Laboratory of Fine Chemicals, Dalian University of Technology, 288#, Linggong Road 2, Dalian 116024, China

Received 30 July 2006; revised 2 October 2006; accepted 2 October 2006

Available online 27 October 2006

Abstract

Intermediate species formed on ZSM-5 zeolites during the selective catalytic reduction of NO by acetylene (C₂H₂-SCR) were investigated by transmittance FTIR and temperature-programmed desorption, to elucidate the different catalytic performance of the proton and sodium forms of ZSM-5. Bidentate nitrates formed exclusively on HZSM-5 were very active toward the reductant, whereas the nitrates associated with the Na⁺ ions on NaZSM-5 were inert. Although the saturation adsorption amount of acetylene on NaZSM-5 was about five times higher than that on HZSM-5 at 80 °C, most of the acetylene on NaZSM-5 was desorbed below 200 °C, whereas a considerable amount of acetylene was detected above 250 °C on HZSM-5 in TPD. The strongly adsorbed species formed on acetylene adsorption was vinyl alcohol (CH₂=CH–OH) bound to the Brønsted acid sites that could be converted to acetate species at elevated temperatures on HZSM-5. Based on our results, a mechanism of the C₂H₂-SCR on HZSM-5 was proposed in which the bidentate nitrates and acetate species formed exclusively on HZSM-5 react with each other, leading to NO_x elimination, which explains why the behavior of HZSM-5 is quite different from that of NaZSM-5 in the C₂H₂-SCR.

© 2006 Published by Elsevier Inc.

Keywords: Proton; Acetylene; Vinyl alcohol; Nitrates; Acetate; ZSM-5; FTIR

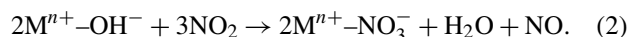
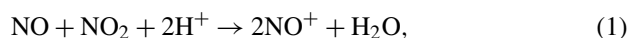
1. Introduction

Selective catalytic reduction of NO by hydrocarbons (HC-SCR) is believed to be the most promising way to remove nitric oxide from the exhaust gas of diesel and lean-burn engines. Since HC-SCR was reported in the presence of excess oxygen over Cu-ZSM-5 [1,2], many studies were carried out in this field both on the catalyst performance and on the reaction mechanism. Hamada et al. [3] reported that catalyst acidity is one of the important factors controlling the catalytic activity for C₃H₈-SCR. Such an effect was also found in the CH₄-SCR on Pd- [4] and Ga-based [5,6] ZSM-5 catalysts. Using propene or propane as a reducing agent, a relationship was found between the population of Brønsted acid sites and the selectivity to NO removal over Pt/aluminum-silicate [7] and over the support alone [8]. A similar dependency was also found in the C₃H₆-SCR over Na-H-MOR [9].

General agreement has evolved that NO oxidation to NO₂ is the initial step of the HC-SCR, and protons have been proposed

as the catalytic sites for NO oxidation [10]. Subsequently, NO₂ is converted to N₂ via a series of reactions:

- (i) NO₂ interacts with the Brønsted acid sites to form NO⁺ [11] through reaction (1) [12] or interacts with hydroxyl groups attached to extra-framework alumina species of zeolites to form nitrates through reaction (2) [13].
- (ii) Hydrocarbon is activated at the Brønsted acid sites [11].
- (iii) Nitrates react with the hydrocarbon or its derivatives to form intermediates, such as nitro-compounds [14], isocyanates [15,16], cyanides [17,18], and amines [11].
- (iv) The intermediates react with gaseous or adsorbed NO_x to form N₂,



In our previous study [19], we found that high NO conversion to N₂ (71.4%) was obtained over HZSM-5 in C₂H₂-SCR, while no activity of NaZSM-5 was detected. In the present article, we report a possible mechanism of C₂H₂-SCR over HZSM-5 based on the role of protons in the catalytic reaction.

* Corresponding author. Fax: +86 411 8363380.
E-mail address: dllgwpx@dlut.edu.cn (X. Wang).

2. Experimental

2.1. Catalysts

Commercial HZSM-5 and NaZSM-5 zeolites ($\text{SiO}_2/\text{Al}_2\text{O}_3 = 25$), purchased from Nankai University, were used in this study. The zeolite samples were calcined at 500°C in air for 6 h and then pelletized, crushed, and sieved to 20–40 mesh before use.

2.2. Activity test of NO oxidation

The activity test of catalysts for NO oxidation was conducted in a quartz reactor (4 mm i.d.) with 0.2 g of catalyst. The gas mixture of 200 ppm NO and 10% O_2 in N_2 was fed to the reactor at a total flow rate of 100 ml/min. The NO_2 produced and unreacted NO in the outlet of the reactor were monitored by an electrochemical NO_x analyzer (ACY301-B).

2.3. NO_x adsorption and TPD

NO_x adsorption and temperature-programmed desorption (TPD) in N_2 were measured in a setup with the ACY301-B analyzer. A sample (0.2 g) pretreated on-line at 550°C in N_2 was first exposed to a gas mixture of 200 ppm NO and 10% O_2 in N_2 at 40°C with a total flow rate of 100 ml/min until saturated adsorption. After N_2 purge (50 ml/min for 2 h), the TPD was carried out from 40 to 500°C with a temperature ramp of $10^\circ\text{C}/\text{min}$.

2.4. C_2H_2 adsorption and TPD

The adsorption of acetylene on the catalysts was performed at 80°C in a quartz reactor on line connected to a gas chromatograph. A catalyst sample (0.2 g) pretreated in N_2 at 500°C was exposed to a gas mixture of 2254 ppm C_2H_2 in N_2 at 80°C with a flow rate of 30 ml/min, during which the concentration of acetylene in the outlet was recorded constantly until saturation adsorption. After purging with N_2 at a flow rate of 30 ml/min for 1 h, the C_2H_2 -TPD was recorded from 80 to 500°C with a temperature ramp of $10^\circ\text{C}/\text{min}$.

2.5. Fourier transform infrared spectroscopy

The in situ FTIR studies were carried out in a quartz IR cell equipped with CaF_2 windows on a Nicolet 360 FTIR spectrophotometer. All of the spectra were obtained by accumulating 32 scans at a resolution of 2 cm^{-1} . The gas mixtures involved in the experiments are given in Table 1, and the adsorption arising from the gases in the cell on the IR laser pathway were recorded at room temperature (coded as S_g). For each experiment, the self-supporting wafer of the zeolite was first activated in situ at 500°C in N_2 , and then its absorption (coded as S_c) was measured at each desired temperature. The IR spectra of surface species in various gas mixtures shown in the figures were obtained by subtracting S_g and S_c from each spectrum.

Table 1
Composition of gas mixtures used in FTIR

No.	Gas mixture	Concentration
1	N_2	Pure nitrogen (99.995%)
2	NO	1000 ppm NO/ N_2
3	C_2H_2	500 ppm $\text{C}_2\text{H}_2/\text{N}_2$
4	NO + O_2	1000 ppm NO + 10% O_2/N_2
5	C_2H_2 + O_2	500 ppm C_2H_2 + 10% O_2/N_2
6	NO + C_2H_2 + O_2	1000 ppm NO + 500 ppm C_2H_2 + 10% O_2/N_2

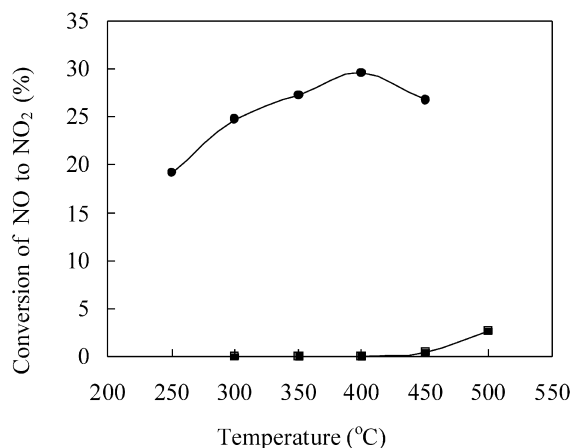


Fig. 1. Catalytic performance of the HZSM-5 (25) and NaZSM-5 (25) catalysts for oxidation of NO with O_2 : HZSM-5 (●) and NaZSM-5 (■) (reaction conditions: 200 ppm NO, 10% O_2 in N_2 , with a total flow rate of 100 ml/min over 0.2 g catalyst).

Desorption of nitrous species formed on the catalysts by exposure to NO and O_2 at 40°C was also monitored by FTIR at 40 – 400°C in N_2 . After NO and O_2 preadsorption, the reactivity of the species toward C_2H_2 was measured by exposing to a gas mixture of C_2H_2 and O_2 in N_2 at 250°C .

The evolution of the carbonous species formed on the catalyst by exposure to C_2H_2 at 80°C was recorded by FTIR at 80 – 410°C in a flow of N_2 . The reactivity of the carbonous species toward NO + O_2 was studied at 200°C in a flow of NO + O_2/N_2 .

Step-response experiments were performed over catalysts at 250°C in the following sequence:

1. Pulsing in 1000 ppm NO + 500 ppm C_2H_2 + 10% O_2/N_2 , followed by brief evacuation.
2. Turning off C_2H_2 (in a 1000 ppm NO + 10% O_2/N_2 flow).
3. Turning off NO and adding C_2H_2 (in a 500 ppm C_2H_2 + 10% O_2/N_2 flow).

3. Results and discussion

3.1. NO oxidation

The activity of the HZSM-5 and NaZSM-5 catalysts in the NO oxidation to NO_2 as a function of temperature shows that HZSM-5 exhibited a high activity in the whole temperature range, whereas almost no conversion of NO was observed over NaZSM-5 (Fig. 1). This indicates that protons are indispens-

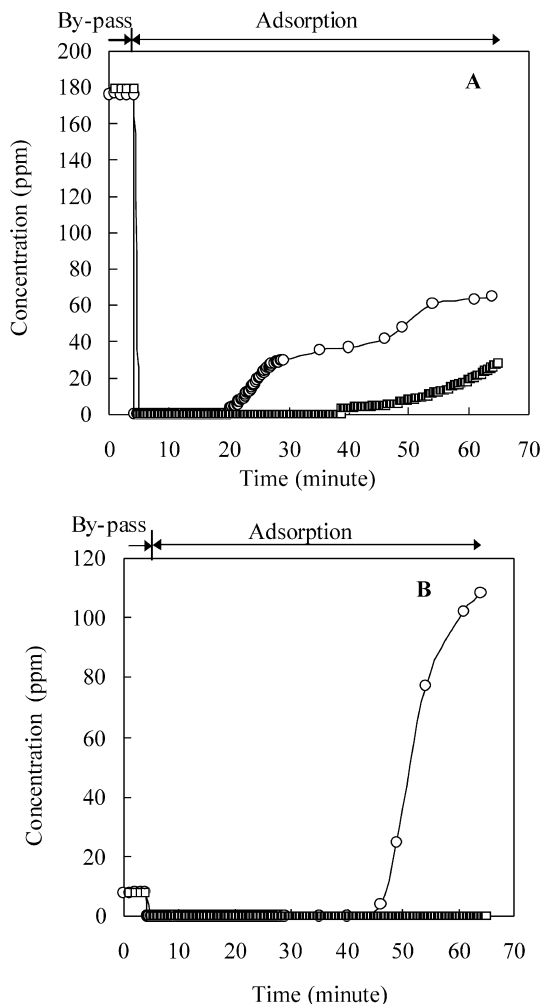


Fig. 2. Adsorption profiles of NO (A) and NO₂ (B) in the co-adsorption of NO with O₂ on HZSM-5 (○) and NaZSM-5 (□) at 40 °C.

able for NO oxidation, as was also found in the CH₄-SCR over Ga- and In-ZSM-5 [6]. This finding, along with the results of the C₂H₂-SCR [19], demonstrates that NO oxidation to NO₂ is an important step of the reaction and that protons in the catalyst are crucial for the C₂H₂-SCR.

3.2. NO and O₂ co-adsorption and TPD

The co-adsorption of NO and O₂ over HZSM-5 and NaZSM-5 (Fig. 2) showed that NaZSM-5 had a higher adsorption capacity for NO_x than HZSM-5. This indicates that Na⁺ ions in the zeolite are favorable for the NO_x storage under the experimental conditions, in line with the results obtained on mordenite zeolite by Satsuma et al. [20]. The promotional effect of Na⁺ on NO_x storage was also observed in the subsequent TPD of NO and NO₂ (Fig. 3). In addition, it is obvious that different nitrous species were formed on HZSM-5 and NaZSM-5, corresponding to the NO₂ desorption peaks at ca. 340 °C (peak A) and ca. 410 °C (peak B), respectively. It seems that protons in HZSM-5 are associated with peak A, whereas Na⁺ in the NaZSM-5 results in peak B, which is discussed further in Section 3.4.1.

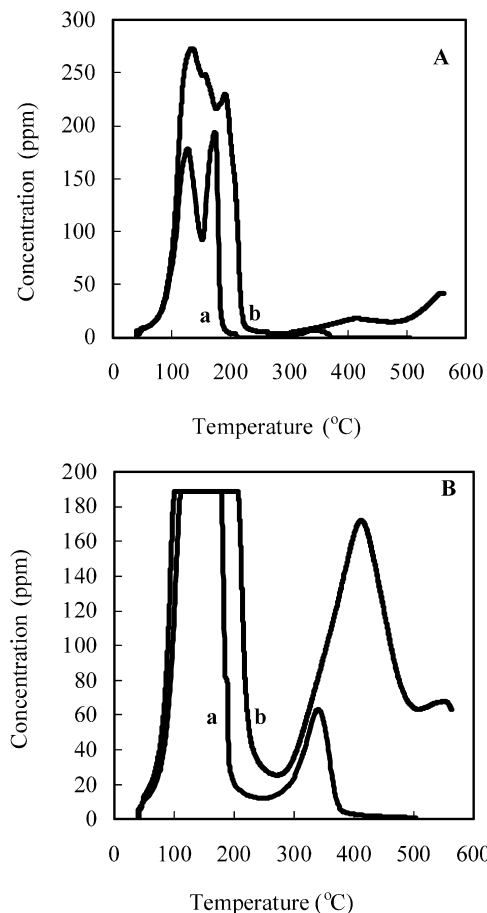


Fig. 3. TPD profiles of NO (A) and NO₂ (B) in N₂ flow after co-adsorption of NO with O₂ on HZSM-5 (a) and NaZSM-5 (b).

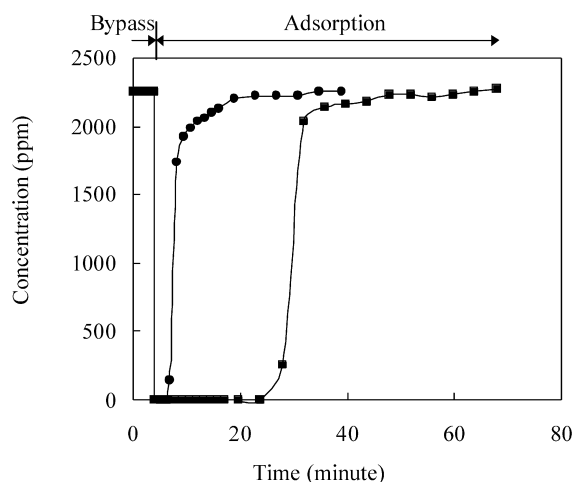


Fig. 4. Time dependence of acetylene concentration upon exposing the HZSM-5 (●) and NaZSM-5 (■) catalysts to 2254 ppm C₂H₂ at 80 °C.

3.3. C₂H₂ adsorption and TPD

The adsorption profiles of acetylene over NaZSM-5 and HZSM-5 at 80 °C show that much more acetylene was adsorbed on NaZSM-5 (0.37 mmol/g) than on HZSM-5 (0.08 mmol/g) in saturation under 2254 ppm C₂H₂ in N₂ (Fig. 4). However, most of it was lost during the subsequent flushing or desorbed

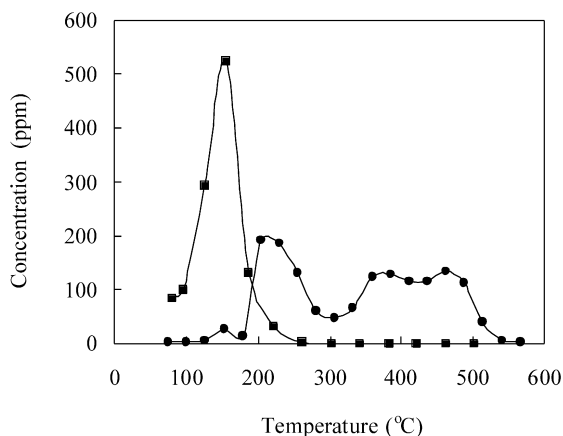


Fig. 5. Temperature-programmed desorption profiles of acetylene from HZSM-5 (●) and NaZSM-5 (■) in a carried gas of N₂ with a flow rate of 30 ml/min.

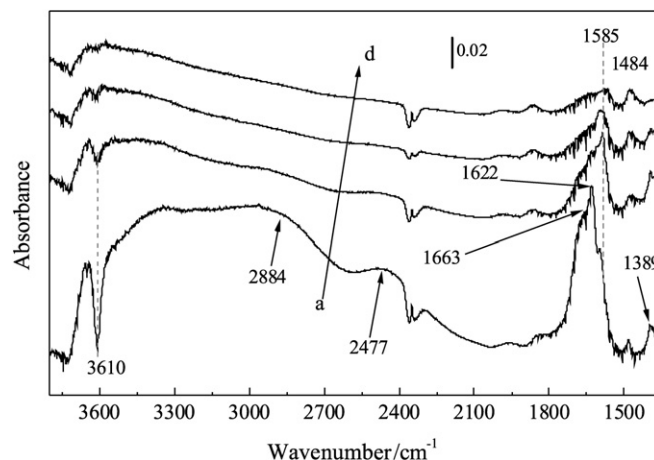


Fig. 7. The variation of nitrous species with temperature on HZSM-5: (a) 150, (b) 250, (c) 350, and (d) 400 °C.

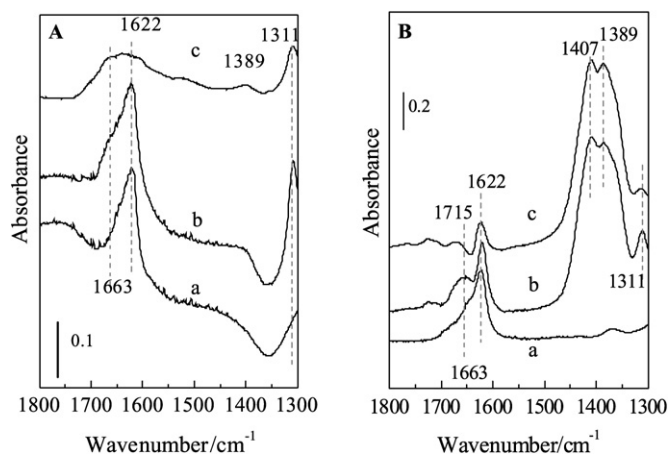


Fig. 6. FTIR spectra of adsorbed species in 1000 ppm NO and 10% O₂ in N₂ at 40 °C on HZSM-5 (A) and NaZSM-5 (B): (a) 1 min, (b) in saturated adsorption, (c) after a brief evacuation.

below 200 °C (Fig. 5), indicating that there is only weak interaction between the acetylene and NaZSM-5. In contrast, although less acetylene was adsorbed on HZSM-5 in saturation, most of it was desorbed above 200 °C (Fig. 5), implying that protons were involved in the strong adsorption of acetylene on the ZSM-5 zeolite.

3.4. In situ FTIR studies

3.4.1. Characteristic of nitrous species formed on the zeolites

The formation of nitrous species and their variation with temperature, as well as their reactivity toward reduction by acetylene, were investigated by FTIR. The spectra obtained on exposure of activated HZSM-5 and NaZSM-5 to NO and O₂ at 40 °C are depicted in Fig. 6. For HZSM-5 (Fig. 6A), the band at 1622 cm⁻¹ due to weakly adsorbed NO₂ [21,22] or bridging nitrates [23–27] and that at 1311 cm⁻¹ due to unidentate nitrates [21,28,29] were observed after the zeolite was exposed to NO and O₂ for 1 min accompanied with three negative bands. The band at 3700 cm⁻¹ was due to the asymmetric stretching vibration of molecular adsorbed water [30,31], and the bands at 2884

and 2477 cm⁻¹ were due to the well-known A–B–C structure produced by hydrogen-bonded hydroxyls [29,31]. The results indicate that the formation of nitrates occurred at the expense of molecular adsorbed water through reaction [24,25,32]:



Further exposure led to an increase in intensity only at 1311 cm⁻¹, which can be explained by reaction (4) being operative on cation defect sites such as extra-framework alumina, similar to the reaction pathway suggested by Larsen et al. [24],



Part of the nitrous species (adsorbed NO₂ and some unidentate nitrates) corresponding to the bands at 1622 and 1311 cm⁻¹ were so weakly adsorbed on the zeolite that they disappeared in the subsequent brief evacuation. At the same time, two bands at 1663 and 1389 cm⁻¹ were observed, which were assigned to the nitrites and/or nitrates associated with a very low concentration of Na⁺ ions in HZSM-5 [20,24,25,33].

Identical to HZSM-5, the band at 1622 cm⁻¹ appeared rapidly with NO and O₂ co-adsorption on NaZSM-5 (Fig. 6B). However, different from HZSM-5, further exposure of NaZSM-5 to NO and O₂ primarily resulted in bands at 1407 and 1389 cm⁻¹ due to nitrates associated with Na⁺ [20,24,25,33]. Fig. 6 clearly shows that more nitrous species were formed on NaZSM-5 than on HZSM-5, which could be well explained by reaction (3), because the NaZSM-5 can hold more molecular water [34]. These results are qualitatively and quantitatively in good agreement with the ones obtained in Section 3.2.

The thermal stability of the nitrous species thus formed on the zeolites was investigated by elevating the temperature in N₂ flow. On HZSM-5, the band at 1311 cm⁻¹ corresponding to the unidentate nitrates disappeared at 150 °C (Fig. 7), and a band appeared at 1585 cm⁻¹ due to bidentate nitrates [21,26–28,35]. This indicates that the bidentate nitrates were formed from unidentate nitrates at the elevated temperature. Compared with the bridging nitrates (1622 cm⁻¹), the bidentate nitrates (1585 cm⁻¹) were more thermally stable; the intensity

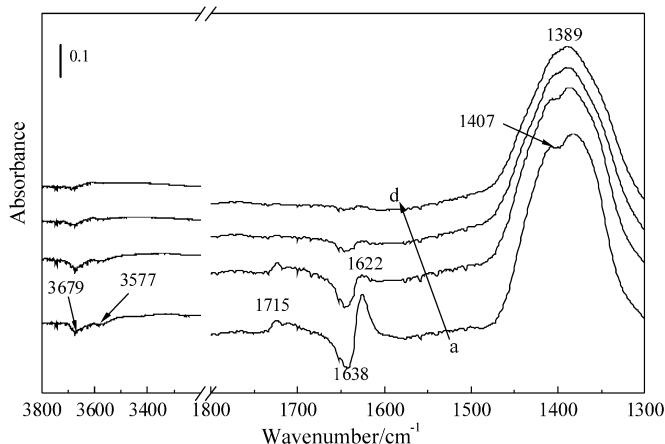


Fig. 8. The variation of nitrous species with temperature on NaZSM-5: (a) 150, (b) 250, (c) 350, and (d) 400 °C.

at 1585 cm^{-1} decreased only slightly with increasing temperature.

Similar to HZSM-5, the unidentate nitrates (1311 cm^{-1}) formed on NaZSM-5 disappeared at 150 °C (Fig. 8), indicating that the unidentate nitrate species is less thermally stable than other kinds of nitrates, irrespective of the adsorbent. This implies that the unidentate nitrates are not involved in the C_2H_2 -SCR (conducted above 250 °C). Quite different from the findings of HZSM-5 (Fig. 7), although the bridging nitrates on NaZSM-5 corresponding to the band at 1622 cm^{-1} changed little below 150 °C , most of them desorbed when the temperature increased to 250 °C (Fig. 8b), corresponding to the large release of NO_x shown in Fig. 3. The band at 1715 cm^{-1} , observed exclusively on NaZSM-5, could be assigned to nitrates associated with Na^+ ions, because it appeared concomitantly with the band at 1407 cm^{-1} during the co-adsorption of NO and O_2 (Fig. 6B) and disappeared at 350 °C together with the same band (Fig. 8c). On NaZSM-5, the most stable nitrous species are the nitrates associated with Na^+ (1389 cm^{-1}), which re-

mained on the zeolite at 400 °C (Fig. 8d), corresponding to the desorption peak above 400 °C (Fig. 3).

The FTIR results, coupled with those reported in Section 3.2, reveal that the adsorption of NO_x on ZSM-5 was strongly affected by the cations in the zeolite, and that protons were essential for the formation of bidentate nitrates.

The bands at 1626 and 1585 cm^{-1} that appeared during co-adsorption of NO and O_2 disappeared within 1 min on exposure of HZSM-5 to C_2H_2 and O_2 at 250 °C (Fig. 9A). Concomitantly, the bands at 1693 cm^{-1} due to carbonyl-containing compound [$\nu(\text{C}=\text{O})$] and at 1605 cm^{-1} due to the $\text{C}=\text{O}$ vibration of carboxylic groups [24] appeared. This indicates that the bridging and bidentate nitrates were very active toward the reductant. No significant change in the spectra was observed when the sample was exposed C_2H_2 and O_2 at 250 °C (Fig. 9B), implying that the nitrates associated with Na^+ on NaZSM-5 were inert to the reductant.

The quite different nitrous species formed on HZSM-5 and on NaZSM-5 as well as their various reactivities toward the reductant, could explain the distinct catalytic performance of the two catalysts in C_2H_2 -SCR. Accordingly, it is rational to draw the conclusion that protons are responsible for the formation of active nitrate intermediates in the C_2H_2 -SCR; that is, protons are essential for NO reduction by acetylene.

3.4.2. Characteristic of carbonous species formed on the zeolites

The evolution of carbonous species and their reactivity toward NO_x were investigated by FTIR. The IR spectra of carbonous species obtained after saturated adsorption of acetylene on the HZSM-5 and NaZSM-5 at 80 °C are depicted in Fig. 10. The adsorption of acetylene on HZSM-5 resulted in the appearance of positive bands at 1673 and 1628 cm^{-1} and negative bands at 3700 , 2884 , and 2477 cm^{-1} (Fig. 10c). As discussed in Section 3.4.1, the three negative bands arose from the consumption of adsorbed water on the Brønsted acid site. No negative band at 3610 cm^{-1} , corresponding to the consumption of acidic

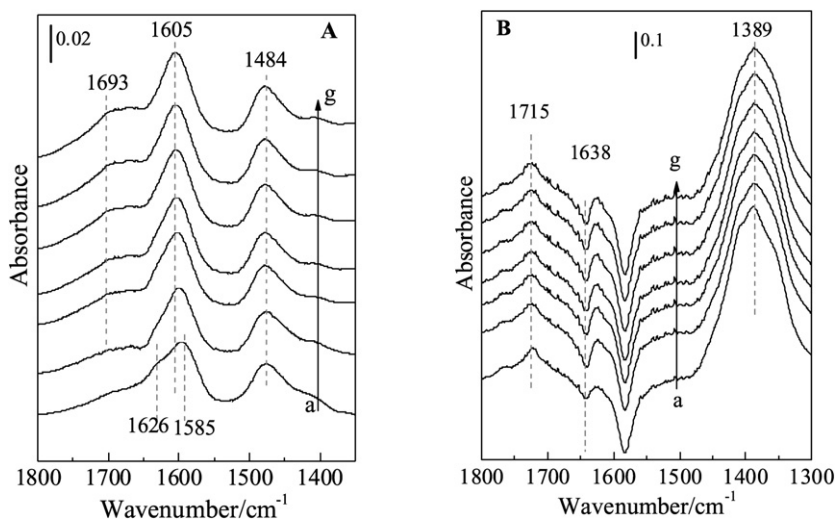


Fig. 9. FTIR spectra on HZSM-5 (A) and NaZSM-5 (B) at 250 °C : (a) brief evacuation after saturation adsorption of NO and O_2 , and subsequently exposing to $\text{C}_2\text{H}_2 + \text{O}_2$: (b) 1, (c) 2, (d) 4, (e) 6, (f) 8, and (g) 10 min.

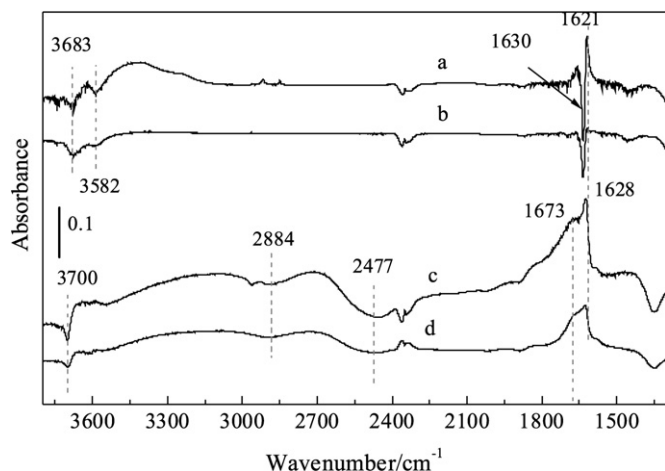
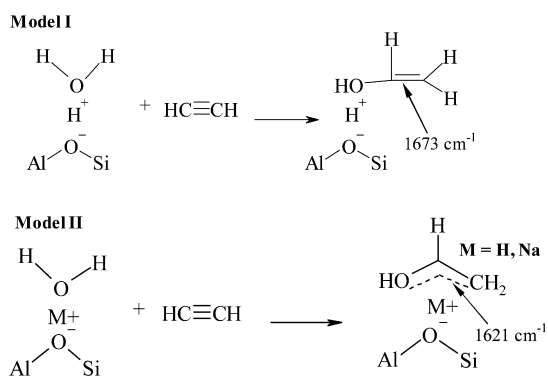


Fig. 10. FTIR spectra of carbonous species formed on the zeolite (a) NaZSM-5, (c) HZSM-5 by saturation adsorption of C_2H_2 at $80^\circ C$ in 500 ppm C_2H_2/N_2 , and subsequent evacuation at $80^\circ C$: (b) NaZSM-5, (d) HZSM-5.



Scheme 1. The C_2H_2 adsorption model on the HZSM-5 and NaZSM-5.

zeolite Al(OH)Si hydroxyls [35,36], was observed on acetylene adsorption. From an energy standpoint, acetylene would adsorb on the free Brønsted acid sites, which were detected on the self-supporting wafer before acetylene adsorption, rather than adsorb on the ones taken up by water. Therefore, we propose that acetylene reacted with the adsorbed water on the Brønsted acid site, but did not simply take up the Brønsted acid site by breaking the well-known A–B–C structure.

Based on the result of the reaction of acetylene with water adsorbed on the Brønsted acid sites, we propose that vinyl alcohol ($CH_2=CH-OH$) was formed on HZSM-5. Vinyl alcohol can adsorb on the ZSM-5 zeolites in two ways (Scheme 1), through strong binding to the Brønsted acid sites with a hydrogen bond corresponding to the band at 1673 cm^{-1} and by binding to the cations (e.g., H^+ and Na^+) in zeolite channels through weak static attraction, corresponding to the band at 1628 cm^{-1} . For vinyl alcohol, the electron-withdrawing action of the $-OH$ group results in a blue shift of $\nu(C=C)$ with respect to the general $C=C$ double band. The blue shift of $\nu(C=C)$ is further aggravated by the hydrogen bond of the $-OH$ group with the Brønsted acid sites (model I). In model II, formation of a π -complex decreases the electron density in the highest occupied molecular orbital, leading to a red shift of $\nu(C=C)$ in vinyl alcohol.

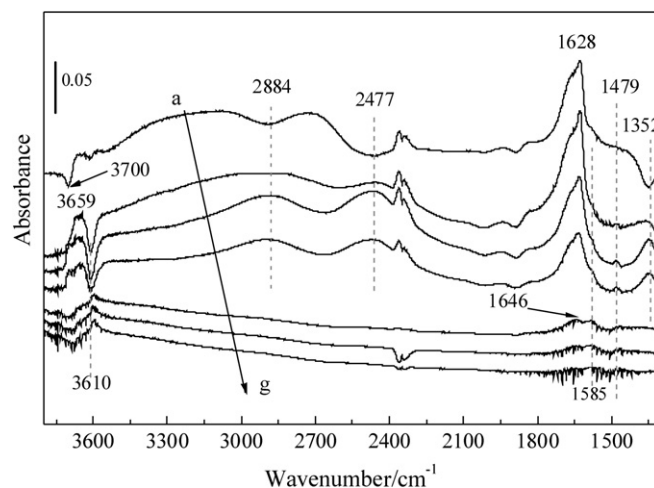


Fig. 11. The spectra of carbonous species on HZSM-5 at the various temperatures: (a) evacuation at $80^\circ C$ after saturation adsorption; (b) 150, (c) 178, (d) 200, (e) 300, (f) 360, and (g) $410^\circ C$.

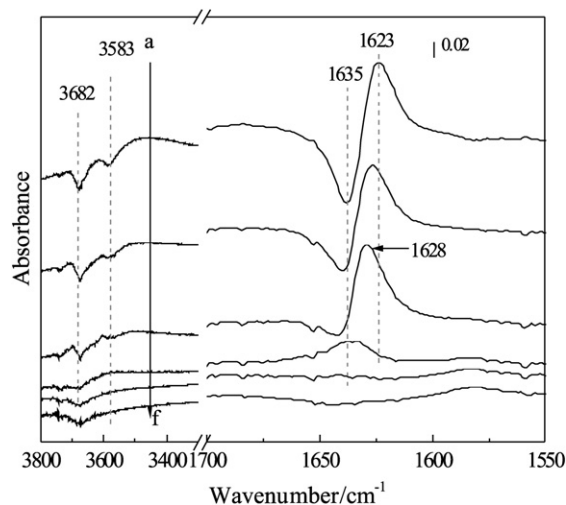
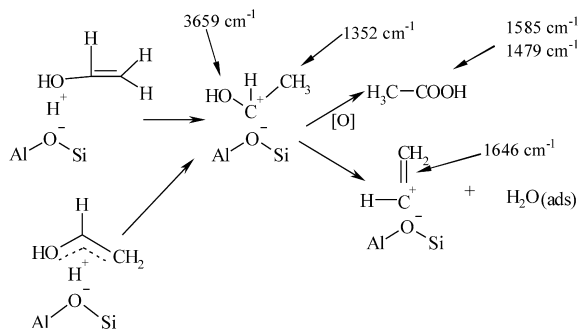


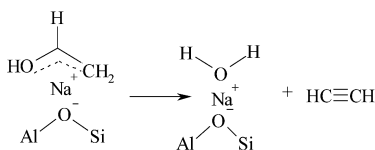
Fig. 12. The spectra of carbonous species on NaZSM-5 at the various temperatures: (a) 150, (b) 178, (c) 200, (d) 300, (e) 360, and (f) $410^\circ C$.

However, only the weakly adsorbed surface species, corresponding to the band at 1621 cm^{-1} , were formed during acetylene adsorption over NaZSM-5 (Fig. 10). The results reported in Section 3.3 indicate that most of the acetylene was adsorbed on the NaZSM-5 with weak interaction. Similar to the case of HZSM-5, the adsorption of acetylene on NaZSM-5 also occurred at the expense of adsorbed water, corresponding to the negative bands at 3683, 3582, and 1635 cm^{-1} [37,38].

Evolution of the carbonous species on HZSM-5 and NaZSM-5 with temperature is shown in Figs. 11 and 12, respectively. It is obvious that the intensity of the bands at 3659 cm^{-1} due to $\nu(-OH)$ of alcohol hydroxyl groups increased with a temperature increase from 80 to $150^\circ C$. At the same time, the bands at 2884 and 2477 cm^{-1} due to the A–B–C structure, and the band at 1352 cm^{-1} due to $\delta(OH)$ of the H-bonded zeolite hydroxyls were recovered on the HZSM-5 (Fig. 11), accompanied by the appearance of the negative band at 3610 cm^{-1} . With further temperature increase, the bands relating to the



Scheme 2. The evolution of carbonous species on HZSM-5.



Scheme 3. The decomposition of carbonous species formed on NaZSM-5.

adsorbed water on the Brønsted acid sites increased in intensity. This indicates that water was formed and adsorbed on the Brønsted acid sites at elevated temperatures. Above 300 °C, the strong band centered at 1628 cm⁻¹ disappeared, which correlates well with the end of desorption peak (around 215 °C) of acetylene in C₂H₂-TPD (Fig. 5). As a result, a new band at 1646 cm⁻¹ was clearly observed. Based on these results, we propose Scheme 2 for the evolution of carbonous species with temperature on HZSM-5.

The vinyl alcohol adsorbed on the Brønsted acid sites in the both models I and II was converted to a carbenium ion (HO-CH⁺-CH₃), which gave bands at 3659 and 1352 cm⁻¹ due to the OH stretching vibration and the CH₃ deformation vibration, respectively. The carbenium ion decomposed to water and another carbonium ion (CH₂=HC⁺) that gave the band at 1646 cm⁻¹. The formed water adsorbed on the Brønsted acid sites led to a recovery of intensity and an increase of

the bands at 2884 and 2477 cm⁻¹, as well as the negative band at 3610 cm⁻¹. In addition, some of the carbenium ion (HO-CH⁺-CH₃) was oxidized by oxygen (ca. 5000 ppm) in the pure N₂ (99.995%) to acetate species, giving the bands at 1585 and 1479 cm⁻¹ due to the ν_{as}(COO) and ν_s(COO) of acetate species [21,26,28,38].

For NaZSM-5 (Fig. 12), a temperature increase from 80 to 200 °C resulted in recovery of the band at 1635 cm⁻¹ as well as a shift of the band (from 1623 to 1628 cm⁻¹). Scheme 3 explains that acetylene was released by the decomposition of vinyl alcohol, leaving water on the cation sites in zeolite, leading to the disappearance of the negative band. Thus the band of vinyl alcohol on sodium ions kept its apparent intensity while it shifted back to its maximum absorption at 1628 cm⁻¹. Above 300 °C, almost no surface species were detected on NaZSM-5, which is in line with the results obtained in C₂H₂-TPD (Fig. 5).

The reactivity of the carbonous species on HZSM-5 toward NO_x was studied at 200 °C in NO/N₂ and NO + O₂/N₂, respectively. Acetate species (1585, 1479 cm⁻¹) were detected at steady state on the HZSM-5 in NO/N₂ and N₂ (Fig. 13A), indicating that the acetate species could exist in NO/N₂. This means that the acetate species did not react with NO at 200 °C. However, in NO + O₂/N₂, no acetate species could be detected; instead, a new band at 2131 cm⁻¹ appeared. This band could be assigned to ν(C≡N) of cyanide [21,39] produced through the reaction of acetate species with NO_x. It means that the acetate species formed through the oxidation of the carbenium ion (HO-CH⁺-CH₃) on HZSM-5 are active toward nitrous species arising from the co-adsorption of NO and O₂, and thus it is one of the important intermediates in the C₂H₂-SCR.

In contrast to the situation for HZSM-5, although vinyl alcohol (1628 cm⁻¹) was formed on NaZSM-5 (Fig. 13B), no change in the band was observed at 200 °C in NO/N₂ and in NO + O₂/N₂, indicating that the vinyl alcohol connected to the cation sites of NaZSM-5 was rather inert under the reaction conditions.

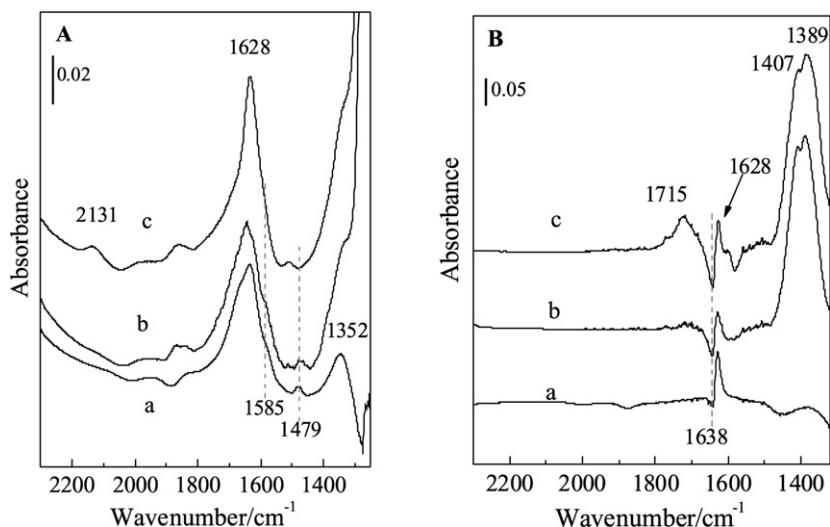


Fig. 13. FTIR spectra of surface species on HZSM-5 (A) and NaZSM-5 (B) at 200 °C taken in (a) N₂, (b) NO, (c) NO + O₂. Before the measurements, the catalysts were pretreated in C₂H₂/N₂ at 80 °C.

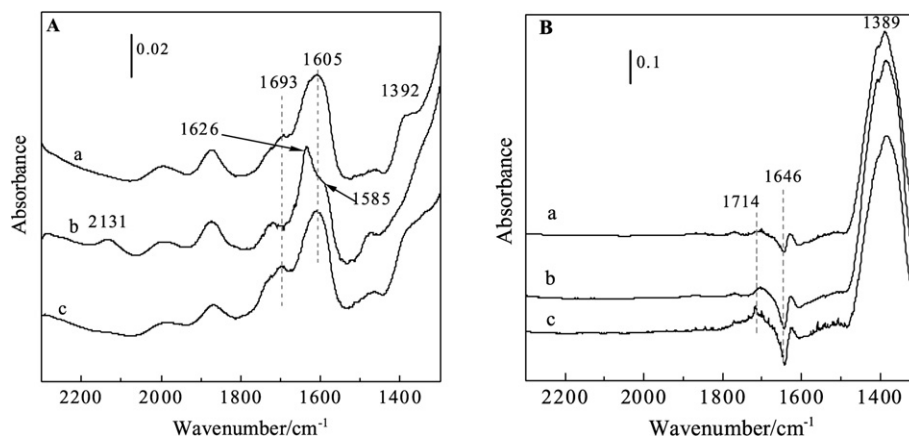
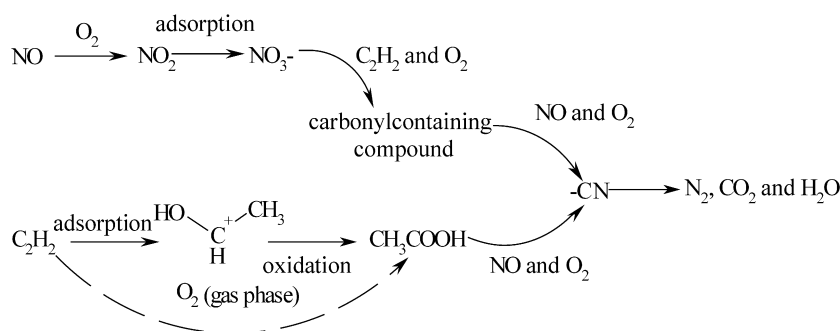


Fig. 14. FTIR spectra on HZSM-5 (A) and NaZSM-5 (B) at 250 °C: (a) evacuation after exposing to NO, C₂H₂ and O₂, followed by (b) exposing to NO and O₂, then by (c) exposing to C₂H₂ and O₂.



3.4.3. Reaction between nitrous species and carbonous species over the zeolites

The FTIR spectrum of surface species on HZSM-5 (Fig. 14 A) was first recorded after a brief evacuation when the C₂H₂-SCR reaction reached steady state (sequence 1: 1000 ppm NO + 500 ppm C₂H₂ + 10% O₂/N₂). As shown in the spectrum a, bands at 1693 and 1605 cm⁻¹, due to carbonyl-containing compound [$\nu(\text{C}=\text{O})$] and the carboxylic groups [$\nu(\text{C}=\text{O})$] [24], respectively, were observed. When acetylene was turned off (sequence 2: 1000 ppm NO + 10% O₂ in N₂), the two bands disappeared, accompanied by the appearance of bands at 1626 (bridging nitrates) and 1585 cm⁻¹ (bidentate nitrates). When NO was turned off and C₂H₂ was added (sequence 3: 500 ppm C₂H₂ + 10% O₂ in N₂), the nitrates and the cyanide species vanished with the reappearance of carbonyl species. The finding that the carbonyl species remained in sequence 1 and disappeared in sequence 2, coupled with the appearance of nitrates only when acetylene was turned off, indicate that the reaction of nitrates with acetylene to form the carbonyl species was a rapid step and that the further reaction of the carbonyl species with nitrates was slower. Similarly, the cyanide species (2131 cm⁻¹) could be observed only when acetylene was cut off, implying that the species reacting with acetylene and/or with its derivatives is fast. The reaction mechanism is summarized in Scheme 4.

No significant change in the spectra of surface species was observed on NaZSM-5 during the three sequences at 250 °C (Fig. 14B). This indicates that the nitrates formed on the

NaZSM-5 were inert toward the reductant in gas phase, because acetylene cannot adsorb on the zeolite at the temperature, as discussed in Section 3.3.

4. Conclusion

Based on our findings, the following conclusions can be drawn:

1. Protons in ZSM-5 zeolites are essential for catalyzing the NO oxidation with O₂ to NO₂, which is the initial step in the SCR of NO by acetylene.
2. Bidentate nitrate species and acetate species, formed exclusively on HZSM-5, are very active toward each other, whereas the nitrates associated with Na⁺ are inert on NaZSM-5. This is why the proton form of ZSM-5 is quite different from the sodium form in the activity for the C₂H₂-SCR.
3. Finally, the function of proton in HZSM-5 can be considered as the sites of (i) catalyzing NO oxidation to NO₂, (ii) adsorbing NO_x to form active nitrates, and (iii) activating acetylene to form active acetate species for the C₂H₂-SCR of NO.

Acknowledgments

The authors thank Professor Can Li, State Key Laboratory of Catalysis, Dalian Institute of Chemical Physics, Chinese Acad-

emy of Sciences, for his help in making the FTIR studies possible. Support was provided by the National Natural Science Foundation of China (grant No. 20677006).

References

- [1] M. Iwamoto, H. Yahiro, Y. Yu-u, S. Shundo, N. Miauno, *Shokubai* 32 (1990) 430.
- [2] W. Held, A. Konig, T. Ritcher, L. Puppe, SAE Paper 900496 (1990).
- [3] H. Hamada, Y. Kintaichi, M. Sasaki, T. Ito, M. Tabata, *Appl. Catal.* 64 (1990) L1.
- [4] Y. Nishizaka, M. Misono, *Chem. Lett.* (1994) 2237.
- [5] Y. Li, J.N. Armor, *J. Catal.* 145 (1994) 1.
- [6] E. Kikuchi, K. Yogo, *Catal. Today* 22 (1994) 73.
- [7] H.H. Ingelsten, M. Skoglundh, E. Fridell, *Appl. Catal. B* 41 (2003) 287.
- [8] H.H. Ingelsten, Å. Hildesson, E. Fridell, M. Skoglundh, *J. Mol. Catal. A* 209 (2004) 199.
- [9] A. Satsuma, K. Shimizu, *Prog. Energy Combust. Sci.* 29 (2003) 71.
- [10] K. Yogo, E. Kikuchi, in: J. Weitkamp, H.G. Karge, H. Pfeifer, W. Hölderich (Eds.), *Zeolites and Related Microporous Materials; State of the Art 1994*, in: *Stud. Surf. Sci. Catal.*, vol. 84, Elsevier, Amsterdam, 1994, p. 1547.
- [11] H.H. Ingelsten, D. Zhao, A. Palmqvist, M. Skoglundh, *J. Catal.* 232 (2005) 68.
- [12] T. Gerlach, F.W. Schütze, M. Baerns, *J. Catal.* 185 (1999) 131.
- [13] U. Bentrup, A. Brückner, M. Richter, R. Fricke, *Appl. Catal. B* 32 (2001) 229.
- [14] H. Imai, T. Ogawa, K. Sugimoto, M. Kataoka, Y. Tanaka, T. Ono, *Appl. Catal. B* 55 (2005) 259.
- [15] F.C. Meunier, V. Zuzaniuk, J.P. Breen, M. Oisson, J.R.H. Ross, *Catal. Today* 59 (2000) 287.
- [16] F.C. Meunier, J.P. Breen, V. Zuzaniuk, M. Oisson, J.R.H. Ross, *J. Catal.* 187 (1999) 493.
- [17] L.J. Lobree, A.W. Aylor, J.A. Reimer, A.T. Bell, *J. Catal.* 169 (1997) 188.
- [18] A.T. Bell, *Catal. Today* 38 (1997) 151.
- [19] X. Wang, Y. Xu, S. Yu, C. Wang, *Catal. Lett.* 103 (2005) 101.
- [20] A. Satsuma, K. Yamada, K. Sato, K. Shimizu, T. Hattori, Y. Murakami, *Catal. Lett.* 45 (1997) 267.
- [21] K. Shimizu, J. Shibata, H. Yoshida, A. Satsuma, T. Hattori, *Appl. Catal. B* 30 (2001) 151.
- [22] G.D. Pirngruber, J.A.Z. Pieterse, *J. Catal.* 237 (2006) 237.
- [23] C. Sedlmair, K. Seshan, A. Jentys, J.A. Lercher, *J. Catal.* 214 (2003) 308.
- [24] G. Li, S.C. Larsen, V.H. Grassian, *Catal. Lett.* 103 (2005) 23.
- [25] G. Li, S.C. Larsen, V.H. Grassian, *J. Mol. Catal. A* 227 (2005) 25.
- [26] Y. Yu, H. He, Q. Feng, H. Gao, X. Yang, *Appl. Catal. B* 49 (2004) 159.
- [27] E. Ivanova, K. Hadjiivanov, D. Klissurski, M. Bevilacqua, T. Armaroli, G. Busca, *Microporous Mesoporous Mater.* 46 (2001) 299.
- [28] H. He, C. Zhang, Y. Yu, *Catal. Today* 90 (2004) 191.
- [29] M. Mihaylov, K. Hadjiivanov, D. Panayotov, *Appl. Catal. B* 51 (2004) 33.
- [30] K. Nakamoto, *Infrared Spectra of Inorganic and Coordination Compounds*, Mir, Moscow, 1996.
- [31] K. Hadjiivanov, J. Saussey, J.L. Freysz, J.C. Lavalley, *Catal. Lett.* 52 (1998) 103.
- [32] J. Szanyi, J.H. Kwak, C.H.F. Peden, *J. Phys. Chem. B* 108 (2004) 3746.
- [33] J. Szanyi, M.T. Paffett, *J. Catal.* 164 (1996) 232.
- [34] J. Szanyi, J.H. Kwak, R.A. Moline, C.H.F. Peden, *Phys. Chem. Chem. Phys.* 5 (2003) 4045.
- [35] F. Poignant, J.L. Freysz, M. Daturi, J. Saussey, *Catal. Today* 70 (2001) 197.
- [36] R. Brosius, P. Bazin, F. Thibault-Starzyk, J.A. Martens, *J. Catal.* 234 (2005) 191.
- [37] U. Bentrup, A. Brückner, M. Richter, R. Fricke, *Appl. Catal. B* 32 (2001) 229.
- [38] Q. Wu, H. He, Y. Yu, *Appl. Catal. B* 61 (2005) 107.
- [39] B.I. Mosqueda-Jiménez, A. Jentys, K. Seshan, J.A. Lercher, *Appl. Catal. B* 46 (2003) 189.